Ultrafast Infrared Spectroscopy

Page O. Stoutland,* R. Brian Dyer, William H. Woodruff

Recent advances in ultrafast infrared spectroscopy are described, including experimental details and fundamental limitations. The utility of this technique is illustrated with two recent examples.

In the course of a chemical reaction, reactants are converted into products with the possibility of various transition states and intermediates on the reaction pathway. The properties of these reactive intermediates and transition-state species are central to the reaction and determine its rate and selectivity. For many years, researchers have used various methods to take "snapshots" of reactions to understand them in more detail. Recently these snapshots have been extended into the picosecond and even femtosecond (10^{-15} s) time regimes, allowing the observation of extremely short-lived intermediates and even species at the transition state (*1*). These observations have obvious fundamental importance in that they allow us to see molecules as they react and to understand the details of the reaction coordinates. In addition, ultrafast dynamics is central to reactions of great practical importance. For example, in the process of vision (*2*) and in the cooperative binding of O_2 to hemoglobin (*3*), ultrafast events are integral parts of transformations for which the overall rate is quite slow.

All of these experiments were made possible by tremendous advances in ultrafast laser technology. These advances have been made in many areas including temporal resolution, sensitivity, wavelength tunability, and, perhaps most important, reliability. Measurement of reaction dynamics on the picosecond and even femtosecond time scales is now common. With the investigation of more complex systems, however, detailed molecular interpretation has become increasingly difficult. For example, most investigations of ultrafast dynamics have been performed by excitation of the sample with a visible "pump," or excitation, pulse, and observation of the changes in the visible region of the spectrum. Unfortunately, for larger and more complex molecules the visible absorption spectrum typically consists of broad, overlapping features from which one can extract little structural information. This difficulty has led to the development of structurally sensitive, ultrafast vibrational spectroscopies that now allow one to gather correlated structural and temporal information on even large, complex systems. In this article we discuss some of the recent advances in ultrafast infrared (IR) spectroscopy with particular attention to applications to chemical systems and illustrate the power of this technique with some recent results from our laboratory (*4*). Space precludes a comprehensive review of the technology; rather, we have chosen to highlight certain aspects central to performing IR spectroscopy on an ultrafast time scale.

The general principles of ultrafast laser experiments are well known. All ultrafast experiments are variants on the "pump-probe" scheme, in which time resolution is obtained by spatial delay of a probe pulse relative to the pump, or excitation, pulse (1 ps = 0.30 mm). Dynamical information is most easily obtained when pump and probe pulses are short compared to the time interval between them. Thus, one needs pulse widths of the same magnitude as the time resolution desired. We will not specifically discuss short-pulse generation but will instead concentrate on details unique to ultrafast IR experiments.

Following the pioneering work of Laubereau and Kaiser (*5*), researchers have performed most ultrafast IR spectroscopy by delaying a short IR pulse of the desired frequency with respect to a pump pulse that is most often in the visible spectrum. Work by Spears *et al.* (*6*), Jedju and Rothberg (*7*), and particularly Heilweil and co-workers (*8*) expanded on early experiments and applied these advances to new chemical systems. Our group, as well, has refined techniques to produce an apparatus that is applicable to many different chemical problems.

Hochstrasser and his co-workers (*9*), however, have pioneered an innovative technique in which a continuous-wave (cw) IR source is used. The cw IR probe beam is passed through the sample where it is overlapped with a femtosecond pump beam. Time resolution is obtained by "gating" the probe beam by upconversion of a temporal slice of it with a second femtosecond visible pulse. This produces a pulse at the sum frequency (IR plus visible) whose intensity is related to the IR absorbance. By changing the temporal delay of this upconversion pulse, one is able to sample different delays relative to the pump beam.

This technique is advantageous in that the upconverted signal is in the visible region where sensitive detectors with very linear responses operate. Additionally, upconversion is intrinsically high resolution because it uses cw IR sources (typically diode lasers or CO gas lasers) that operate on transitions with narrow linewidths. Thus, the resolution is in principle limited only by homogeneous or inhomogeneous broadening intrinsic to the sample (*10*). The single wavelength nature of this approach, however, precludes the possibility of multichannel experiments.

Because upconversion experiments do not involve the generation or detection of IR pulses, the experimental details are very similar to ultrafast experiments in the visible spectrum and will not be discussed here. The upconversion step itself is related to the generation of IR pulses and has been discussed in detail (*11*). The remainder of the discussion will concentrate on the generation and detection of the short IR pulses required to perform ultrafast IR experiments in which a short IR pulse is delayed with respect to a pump pulse.

The starting point for most ultrafast spectroscopies is a short-pulse dye laser, in our case a cw Nd:YAG pumped dual-jet dye laser amplified in a three-stage dye amplifier (Fig. 1). This standard technology has been well described (*12*). All of our experiments were performed with a visible or near-ultraviolet pump pulse and an IR probe pulse. We obtain a tunable pump pulse by focusing the amplified dye pulse into a cuvette of water to produce a continuum, selecting a slice of the continuum with an interference filter, and subsequently amplifying the desired portion in a two-stage amplifier (*13*). Continuum amplification, in combination with nonlinear mixing techniques, thus provides a pump pulse tunable throughout the visible and near-ultraviolet regions.

Generation of Short Infrared Pulses

There are several ways to generate short IR pulses. These are typically based on Raman scattering processes (*14*) or nonlinear mixing schemes (*7*). Most picosecond or femtosecond IR experiments have made use of nonlinear mixing schemes or the related optical parametric oscillator (OPO). Briefly, these techniques make use of the possibility of one photon generating two photons (with conservation of energy and momentum) in a nonlinear crystal under the proper phase-matching conditions. These conditions can be met, for example, in $LiIO_3$, allowing a 532-nm photon to generate a 5-μm (2000 cm^{-1}) photon and a

P. O. Stoutland and R. B. Dyer are in the Division of Chemical and Laser Sciences and W. H. Woodruff is in the Division of Isotope and Nuclear Chemistry at the Los Alamos National Laboratory, Los Alamos, NM 87545.

*To whom correspondence should be addressed.

595-nm photon. In an OPO the desired wavelength (5 μm, in this case) builds up from the noise and is then often used to seed a second crystal. This technique has been demonstrated by Laubereau and coworkers (*15*) in both the picosecond and femtosecond regimes. However, the related method of difference frequency mixing has proven more convenient, especially in the femtosecond regime where group velocity concerns become important. Difference frequency generation is conceptually related to an OPO, but in this case one directly "seeds" the crystal with one of the desired wavelengths. For example, to produce 5-μm light, a 532-nm pulse and a 595-nm seed pulse are directed into the crystal simultaneously to produce a 595-nm photon and a 5-μm photon for every 532-nm photon destroyed. Photon conversion efficiencies are generally on the order of 10% and the resulting pulses have the same pulse width as the shorter of the two pulses. In our experimental setup, we mixed a 75-ps 532-nm pump pulse with a 2-ps seed pulse at ~595 nm. This combination resulted in a ~5-μm pulse of 2-ps duration.

The required phase-matching conditions depend on the crystal type. For type I phase matching in a negative uniaxial crystal (*16*), a photon with its polarization along the extraordinary axis of the crystal splits into two photons with polarizations along the ordinary axis. Changing the angle of the crystal relative to the polarization of the pump photon affects only the refractive index of the extraordinary wave and allows one to achieve phase-matching conditions for a range of colors. With $LiIO_3$ one can generate IR photons from the near-IR region to ~1850 cm^{-1}. The IR wavelength range can be extended below 1850 cm^{-1} by two-stage mixing schemes in which the final stage involves mixing a pulse of 1064 nm, for example, with a 1200- to 1300-nm pulse in $AgGaS_2$ (*17*). Broadband visible seed pulses can generate broadband IR pulses and make multichannel experiments possible (*18*). For a range of wavelengths, care must be taken either to focus the visible seed pulse lightly into the crystal so that phase-matching conditions are met or to use noncritical phase-matching conditions that are less sensitive to wavelength (*19*).

On the picosecond and femtosecond time scales, the pulse-broadening effects of group velocity dispersion (GVD) become significant; in normally dispersive media GVD leads to blue light traveling slower than red light. In difference frequency generation, GVD causes the generated IR photons to "walk away" from the bluer light used to generate the IR. This results in pulse broadening in direct proportion to the length of the crystal and its dispersive properties. Generating IR pulse of 2 ps from a 2-ps 595-nm pulse and a 532-nm pulse thus requires that an $LiIO_3$ crystal, for example, be no more than 5 to 10 mm long (*20*). Pulse broadening directly scales with crystal length, which suggests that to generate 200-fs IR pulses, crystal lengths must be less than 1 mm. As noted earlier, it is possible to generate broad-band IR pulses by seeding the process with a spectrally broad visible source. In these cases, it is also necessary to consider the implications of GVD for the IR pulse itself (*21*).

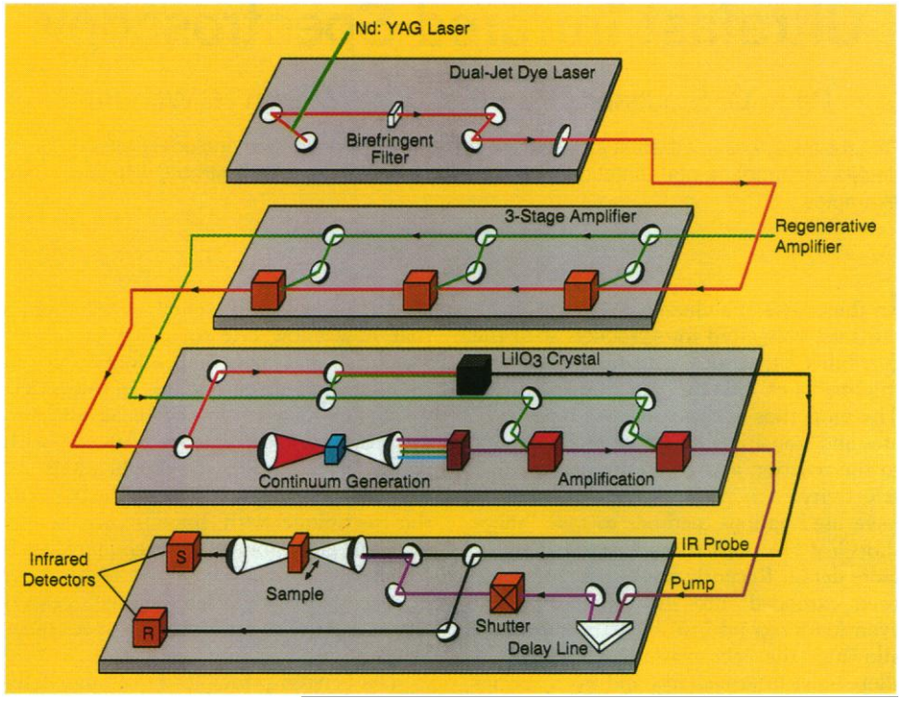

Fig. 1. Schematic of our picosecond time-resolved IR apparatus.

Fundamental Limitations

In the IR spectral region, limits imposed on pulsed signals by the Heisenberg uncertainty principle become particularly significant. For Gaussian-shaped, transform-limited pulses, for example, this requires that the time-bandwidth product, $\tau_{pulse} \cdot \Delta f_{pulse}$, be approximately equal to 0.44. A 200-fs pulse thus has a bandwidth of at least 75 cm^{-1}. There are methods, however, of obtaining spectral resolution limited not by the pulse but by the sample alone. For example, a short, spectrally broad pulse may be sent through the sample and subsequently dispersed in a monochromator to regain the frequency resolution. This approach is successful in that it allows one to obtain frequency resolution that in principle is restrained only by broadening intrinsic to the sample. Beckerle *et al.* (*22*) have verified this in an experiment in which the spectra of gaseous CO were taken with a 730-fs near-transform-limited pulse (Δf_{pulse} ~ 15 cm^{-1}) that was dispersed in a monochromator after passing through the sample. The resulting spectrum had monochromator-limited (<1 cm^{-1}) resolution.

This type of experiment is successful because the short pump pulse induces a polarization field in the sample that subsequently radiates coherently with the probe and decays with the optical dephasing time constant. In the limit where τ_{pulse} < optical dephasing time (T_2), this polarization exists after the probe pulse has formally passed through the sample and is referred to as the free induction decay (*23*). Consequently, the resolution that may be obtained with short, spectrally broad pulses is limited not by the bandwidth of the pulse but by the interaction time of the field with the sample. In the limit, this interaction time is determined by T_2 and is inversely proportional to the resolvable bandwidth. Thus, even with spectrally broad probe pulses, spectra of transient species may be resolved to the extent that their lifetimes (and any inhomogeneous broadening) allow.

Signal-to-Noise Considerations

To provide maximum sensitivity, the probe beam is split into sample and reference beams before it reaches the sample. These are detected by indium antimonide or mercury cadmium telluride detectors cooled to 77 K, which are capable of sensing mid-IR pulses with nanojoule/pulse energies. The ratio of the sample signal to the reference signal is computed electronically. Unfortu-

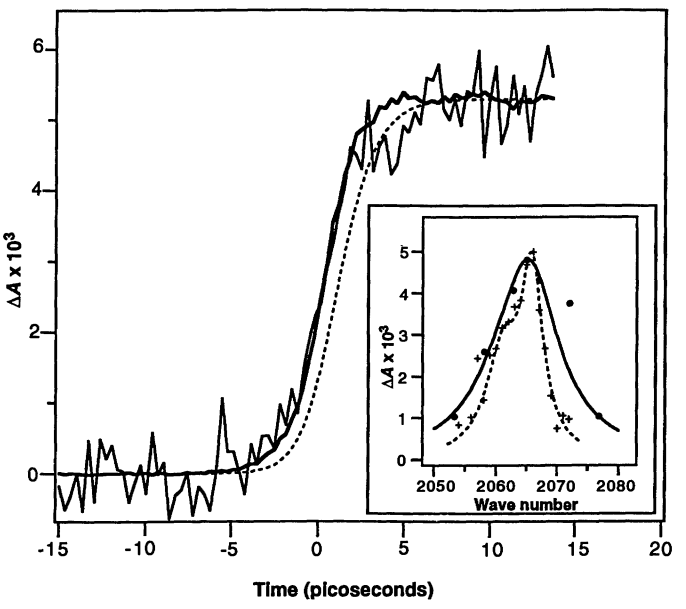

Fig. 2. Transient monitored at the peak of the Cu_B-CO absorption at 2062 cm^{-1}. Each point is the average of ~2000 laser shots. The smooth traces are, leftmost, the experimentally determined instrument response function and, rightmost, the convolution of this function with a 1-ps exponential rise. Inset are spectra determined at 5 ps (solid line) and 100 ns (dashed line, see text). The nanosecond spectrum was normalized to match the ps spectrum.

nately, semiconductor detectors are notoriously nonlinear. In addition to using matched detectors, one must adjust the amount of radiation sent to the signal and reference detectors so that they accurately track one another (*24*). Additionally, we chop our pump beam at one-half the laser repetition rate (30 Hz) to compensate for short-term instabilities and improve the signal-to-noise ratio (S/N) by three to four times. The resulting S/N allows the detection of absorbance changes on the order of 10^{-3} (with an S/N >10) with reasonable signal averaging. Furthermore, the spectral brightness of the probe combined with sensitive detectors allows detection of these small absorbance changes in samples having high background absorbances (optical densities >1.0).

Applications of Ultrafast Infrared Spectroscopy

The chemical applications of IR spectroscopy on the picosecond or femtosecond time scale have expanded to the areas of biophysical chemistry (*25, 26*), organometallic chemistry (*27*), and energy transfer dynamics (*28, 29*). For example, Hochstrasser and co-workers (*25*) have extensively investigated the dynamics after CO dissociation from CO-ligated hemoglobin and myoglobin by monitoring the CO chromophore. These studies have not only provided evidence for the sub-picoseond dissociation of CO but have provided structural information as well. For example, the relative absorbance changes that occur when the probe light is oriented parallel or perpendicular to the pump can be used to extract the angle of the CO transition dipole relative to the excitation transition dipole that lies in the heme plane. In addition, sites in the protein where CO binds weakly after photodissociation have been identified. These results may have implications for the binding of exogenous ligands to heme proteins in general.

Heilweil *et al.* (*28*) have used ultrafast IR spectroscopy to investigate energy transfer dynamics of organometallic molecules both in solution and on surfaces. In these experiments, the pump pulse was also in the mid-IR region and was resonant with an IR absorption in the sample. This process produced a nonequilibrium vibrational population in the resonant mode; the subsequent probe pulse monitored the redistribution of this vibrational population. These experiments have shown that energy transfer out of high-frequency modes (typically MC≡O modes) is slow and depends quite strongly on the medium. Such information is central to understanding chemical activation and how thermally activated reactions occur. Recent experiments have provided complementary information for reactions on surfaces.

To illustrate the versatility of ultrafast IR spectroscopy in more detail, we have chosen two examples from our laboratory where we have used this technique to address problems in biophysical and inorganic chemistry. In biophysical chemistry, we used picosecond IR spectroscopy to investigate the ligand transfer dynamics of bovine cytochrome c oxidase (*30*). This enzyme catalyzes the terminal reaction in the respiratory chain in which O_2 is reduced to H_2O. In the process it stores the redox energy as a transmembrane proton gradient that is subsequently used to generate adenosine triphosphate (*31*). One of the key steps in the reduction of O_2 is its binding to an iron porphyrin site (typically referred to as cytochrome a_3, or Fe_{a_3}). Here oxygen reduction takes place by a stepwise transfer of electrons from other metal centers.

Nanosecond, time-resolved IR experiments with cytochrome c oxidase in which a CO ligand is bound to the Fe_{a_3} site had demonstrated that, upon photodissociation, CO binds within 100 ns to the adjacent copper site (Cu_B) located ~5 Å from the heme center (*32*). Additional experiments implicated a Cu_B-CO intermediate in the reverse reaction as well, suggesting that Cu might have an interesting ligand transfer role in this protein (*33*). We chose to investigate the ps dynamics in the hope of temporally resolving the ligation of CO to the Cu center. This reaction cannot be observed with visible spectroscopy because the Cu(I) center is spectroscopically silent in this region (*34*).

Initial experiments in which the IR probe pulse was tuned to the Fe_{a_3}-C≡O absorbance showed an instrumentally limited decrease in absorbance consistent with the rapid loss of CO after absorption of the 600-nm pump photon. Subsequently, we investigated the dynamics of Cu_B-C≡O absorbance at 2062 cm^{-1} (*30*). Using the known instrumental response (*35*) and deconvolution techniques, we were able to conclude that CO transferred to the Cu site within 1 ps (Fig. 2). Furthermore, by changing the IR probe frequency we saw that the dynamics were independent of wavelength. In addition, we found that the spectrum observed at 1 ps was equivalent to that seen on the nanosecond and longer time scales, broadened by the ~8 cm^{-1} bandwidth of the probe pulse (Fig. 2, inset).

These observations require that photodissociation from Fe_{a_3} occur, CO migrate to the Cu_B site, and formation of the Cu_B-CO bond be complete within 1 ps. This remarkably fast rate indicates that the Fe_{a_3}-Cu_B site is constructed in such a way as to facilitate CO transfer and that energy transfer out of the incipient Cu_B-CO bond is extremely rapid. Models in which "free" CO is formed in the photodissociation and its subsequent motion is considered to be diffusive cannot account for the rapid transfer to the Cu site. In a more plausible model, free CO is not formed but remains in the Fe_{a_3}-Cu_B pocket and is transferred from the Fe to the Cu center in a concerted mechanism. This is consistent with static IR spectra in which the linewidth of the Fe_{a_3}-C≡O transition appears narrow, suggesting a rigid, confined heme pocket. The observation that the Cu_B-C≡O absorbance does not shift at short times indicates that it is formed in its vibrational ground state and that energy transfer from the incipient Cu_B-C bond to the C≡O oscillator must be slow. Conversely, this implies that the protein is able to dissipate the excess energy efficiently. The observed reaction also has general implications. For example, the rapid transfer of CO provides an opportunity to study

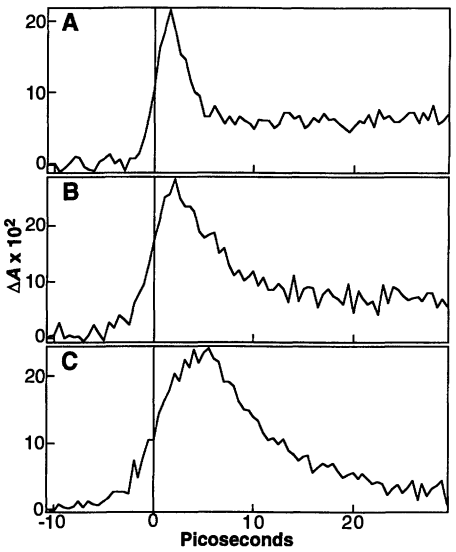

Fig. 3. Transient decays obtained at (**A**) 1954, (**B**) 1994, and (**C**) 2034 cm^{-1} from 0.04 M dimer in D_2O. See Table 1 for appropriate rise and decay times. Offsets remaining at long times are due to thermal transients and do not affect the fits obtained.

bond formation in much the same way that femtosecond visible spectroscopy has recently been used to investigate bond breakage (*1*).

In inorganic chemistry, we are using ultrafast IR spectroscopy to probe the electron transfer dynamics of a series of asymmetric, mixed-valent transition-metal dimers: $[(NC)_5M^{II}CNM^{III}(NH_3)_5]^-$. To date we have most thoroughly investigated the, complex where M represents ruthenium (*36*). This complex is interesting in that the Ru centers are strongly coupled through a short cyanide bridge. However, because the $[(NC)_5Ru^{III}CNRu^{II}(NH_3)_5]^-$ state of this system lies ~8000 cm^{-1} higher in energy, the odd electron is localized on the ruthenium cyanide center (*37*). Optical excitation of the metal-metal charge transfer (MMCT) band with photons of energy $h\nu$ leads to reduction of the ruthenium-amine site. This state is highly unstable with respect to back-electron transfer.

$$[(NC)_5Ru^{II}CNRu^{III}(NH_3)_5]^- \overset{h\nu}{\underset{ET}{\rightleftharpoons}} [(NC)_5Ru^{III}CNRu^{II}(NH_3)_5]^-$$

The MMCT excitation is followed by back-electron transfer (ET), predicted to occur on a very short time scale. We follow the dynamics of this process by observing the stretching frequency of terminal RuC≡N, centered at 2053 cm^{-1} in the ground state [full width at half maximum (FWHM) = 23 cm^{-1}]. This band is sensitive to the charge at the metal center and, because of anharmonicity, to the degree of vibrational excitation of this mode.

Upon excitation at 600 nm (16,670 cm^{-1}), an instrumentally limited (τ < 500 fs) decrease was observed in the RuC≡N absorbance for the ground state at 2053 cm^{-1} that recovered with a time constant of 6 ps. Simultaneously with the ground-state bleach, we observed a new absorption centered at 2110 cm^{-1} that decayed with τ < 0.5 ps. We subsquently saw a broad feature extending from 1950 to 2040 cm^{-1}. Three kinetic traces taken throughout this region are shown in Fig. 3. The rise times of the transients at the low-energy end of the band are instrument limited but become progressively slower when moving to the high-energy side. In fact, they correspond to the decay times found for the lower energy transients (Table 1).

The MMCT excitation should lead to a complex in which the ruthenium cyanide center has formally changed from a 2+ to a 3+ oxidation state. This should result in a shift of the RuC≡N stretch from the ground-state value of 2053 cm^{-1} to ~2120 cm^{-1} (*38*). We thus assign the short-lived transient at 2110 cm^{-1} to the MMCT excited state. The features between 1950 and 2040 cm^{-1} are consistent with vibrationally hot ground-state molecules formed after the back-electron transfer. Metal-cyanide stretching vibrations exhibit anharmonicities of about 14 cm^{-1} (*39*), leading to vibrationally excited states that are shifted to lower energy from the ground-state band. The observed frequencies correspond to population of the vibrationally excited states (v) 1 to 7 (*40*). Pumping with lower energy photons (700 nm = 14,290 cm^{-1}) results in population up to only v = 4. These results are remarkable in that most of the available energy is converted into vibrational excitation of the RuC≡N terminal mode, indicating that this mode is important in coupling the excited state to the ground-state surface (*41*).

Data taken throughout the wavelength range 1950 to 2040 cm^{-1} showed a steady progression of rate constants with higher vibrational states (lower C≡N stretching frequencies) relaxing more quickly. These findings are consistent with the expectation (*42*) that higher vibrational states have larger cross sections for energy transfer. In the present case, relaxation can take place through either an intramolecular mechanism [that is, intramolecular vibrational redistribution (IVR)], transfer of the excess energy to the surrounding solvent molecules, or a combination of the two (*43*). Recent experiments have shown that energy transfer rates are three to four times faster in D_2O than in H_2O and that energy transfer rates are significantly decreased upon substituting osmium for ruthenium. This suggests that both IVR and energy transfer to solvent occur simultaneously in these systems (*44*).

Table 1. Rise and decay times for the best fit to data from 1954 to 2060 cm^{-1}. Best fit obtained during convolution of the instrument response (typically a 3- to 4-ps FWHM $sech^2$ function) with a biexponential function; estimated relative error ±0.5 ps.

Wavelength (cm^{-1})	Rise time (ps)	Fall time (ps)
1954	0.1	0.7
1974	0.3	1.9
1994	0.6	3.6
2014	0.7	4.6
2034	1.4	5.9
2060*	0.0	6.9

*Ground-state bleach.

This study shows the potential of ultrafast IR spectroscopy for studying complex reactions. For example, the IR frequency observed for the RuC≡N stretch in the MMCT state shows that nearly a full charge transfer occurs. Upon a return to the ground electronic state, large amounts of energy (up to 14,000 cm^{-1}) are placed into a single vibration: the terminal RuC≡N stretching mode, with the more highly excited states relaxing more quickly. Finally, the relative rates observed for electronic and vibrational relaxation in $[(NC)_5Ru^{II}CNRu^{III}(NH_3)_5]^-$ suggest that activated modes in the excited state remain so on the time scale of electron transfer. This holds important consequences for electron transfer theories and for fast electron transfer processes such as charge separation in photosynthesis.

Future Directions

To date most ultrafast IR measurements have been made on metal carbonyl or similar compounds because of their large absorption cross section in the IR region. It is now possible to look throughout the IR spectrum on an ultrafast time scale with sensitivities that make possible probing of other vibrational transitions. The low-frequency region in particular is rich in structural information and has yet to be exploited on an ultrafast time scale. It is thus anticipated that, as sensitivities and tunability are further improved, ultrafast IR spectroscopy will find applications in a wide variety of fields where correlated structural and temporal information is required.

REFERENCES AND NOTES

1. For recent reviews, see: A. H. Zewail, *Science* **242**, 1645 (1988); C. V. Shank, *ibid.* **233**, 1276 (1986).
2. R. W. Schoewnlein, L. A. Peteanu, R. A. Mathies, C. V. Shank, *ibid.* **254**, 412 (1991).
3. J. W. Petrich, C. Poyart, J.-L. Martin, *Biochemistry* **27**, 4049 (1988); J. W. Petrich and J.-L. Martin, *Chem. Phys.* **131**, 31 (1989).
4. We have concentrated our efforts on IR spectros-

copy, which has some technological advantages to our applications. For example, ultrafast Raman spectroscopy is difficult to use with photolabile species and often has the required sensitivity only if there is an electronic absorption band resonant with the probe pulse (that is, resonance Raman). fFor a recent example of femtosecond Raman spectroscopy, see (*3*).

5. A. Fendt, W. Kranitzky, A. Laubereau, W. Kaiser, *Opt. Commun.* **28**, 142 (1978); A. Seilmeier, K. Spanner, A. Laubereau, W. Kaiser, *ibid.* **24**, 237 (1978); A. Laubereau, L. Grieter, W. Kaiser, *Appl. Phys. Lett.* **25**, 87 (1974).
6. K. G. Spears, X. Zhu, X. Yang, L. Wang, *Opt. Commun.* **66**, 167 (1988).
7. T. M. Jedju and L. Rothberg, *Appl. Opt.* **27**, 615 (1988).
8. E. J. Heilweil, *Opt. Lett.* **14**, 551 (1989); _____, R. R. Cavanagh, J. C. Stephenson, *Chem. Phys. Lett.* **134**, 181 (1987).
9. J. N. Moore, P. A. Hansen, R. M. Hochstrasser, *Chem. Phys. Lett.* **138**, 110 (1987). For a recent variant of this technique see: T. M. Jedju, M. W. Robinson, L. Rothberg, *Appl. Opt.* **31**, 2684 (1992).
10. Conversely, one of the limitations of the technique is that cw IR sources with sufficient power (several milliwatts) at the desired frequency are needed. This may require multimodal operation of the IR laser with accordingly poorer resolution.
11. For general discussions of experiments using the upconversion technique, see: P. A. Anfinrud, C. Han, T. Lian, R. M. Hochstrasser, *J. Phys. Chem.* **94**, 1180 (1990) and (*9*).
12. For general references, see: G. R. Fleming, *Chemical Applications of Ultrafast Spectroscopy* (Oxford Univ. Press, New York, 1986), *Dye Laser Principles: With Applications*, F. J. Duarte, Ed. (Academic Press, Boston, 1990); A. Migus, C. V. Shank, E. P. Ippen, R. L. Fork, *IEEE J. Quant. Electron* **QE-18**, 101 (1982); I. N. Duling, T. Norris, T. Sizer, P. Bado, G. Mourou, *J. Opt. Soc. Am.* **B2**, 616 (1985). For specific details of our experimental system, see: R. B. Dyer, K. A. Peterson, P. O. Stoutland, W. H. Woodruff, *J. Am. Chem. Soc.* **113**, 6276 (1991); S. K. Doorn, P. O. Stoutland, R. B. Dyer, W. H. Woodruff, *ibid.* **114**, 3133 (1992).
13. The technique of continuum amplification has been well described in: A. Migus, J.-L. Martin, R. Astier, A. Antonetti, A. Orszag, *Picosecond Phenomena* (Springer Series in Chemical Physics, no. 23, New York, 1982), pp. 6–9; A. Migus, A. Antonetti, J. Etchepare, D. Hulin, A. Orszag, *J. Opt. Soc. Am. B Opt. Phys.* **2**, 584 (1985).
14. J. H. Glownia, J. Misewich, P. P. Sorokin, *Opt. Lett.* **12**, 19 (1987).
15. See, for example, R. Laenen, H. Graener, A. Laubereau, *ibid.* **15**, 971 (1990); R. Laenen, H. Graener, H. A. Laubereau, *Proc. SPIE Int. Soc. Opt. Eng.* **1268**, 73 (1990).
16. For a colinear arrangement, $n_p\omega_p = n_s\omega_s + n_i\omega_i$ where n is the refractive index, ω the frequency, and p, s, and i signify the pump, signal, and idler photons in Raman terminology.
17. H.-J. Hübner, M. Wörner, W. Kaiser, A. Seilmeier, *Chem. Phys. Lett.* **182**, 315 (1991); T. Elsässer, H. Lobentanzer, A. Seilmeier, *Opt. Commun.* **52**, 355 (1985).
18. Multichannel IR experiments have been conducted by Heilweil (*8*). In these experiments the broadband IR pulse was upconverted into the visible region and subsequently detected with a multichannel detector. We are developing an alternative approach in which the IR pulse is monitored directly.
19. See, for example, R. J. Seymour and F. Zernike, *Appl. Phys. Lett.* **29**, 705 (1976).
20. Calculated with appropriate refractive indices of $LiIO_3$ [Cleveland Crystals Data Sheet; M. M. Choy and R. L. Byer, *Phys. Rev. B* **14**, 1693 (1976)] using the limits described for minimal pulse broadening in [M. A. Kahlow, W. Jarzeba, T. P. DuBruil, P. F. Barbara, *Rev. Sci. Instrum.* **59**, 1098 (1988)].
21. In principle, it is possible to precompensate for this dispersion by chirping the visible pulse.
22. J. D. Berkerle, R. R. Cavanagh, M. P. Casassa, E. J. Heilweil, J. C. Stephenson, *J. Chem. Phys.* **95**, 5403 (1991).
23. For discussions of free induction decays after optical excitation, see (*22*); J. D. Beckerle, R. R. Cavanagh, M. P. Casassa, E. J. Heilweil, J. C. Stephenson, *Chem. Phys.* **160**, 487 (1992); M. Joffre *et al.*, *Opt. Lett.* **13**, 276 (1988); M. Joffre, D. Hulin, A. Migus, A. Antonetti, *J. Mod. Opt.* **35**, 1951 (1988).
24. It is possible that liquid helium bolometers are more linear and provide a suitably short time response. To our knowledge no one has tested this possibility with ps pulses.
25. J. N. Moore, P. A. Hansen, R. M. Hochstrasser, *Proc. Natl. Acad. Sci. U.S.A.* **85**, 5062 (1988); P. A. Anfinrud, C. Han, R. M. Hochstrasser, *ibid.* **86**, 8387 (1989).
26. T. M. Jedju, L. Rothberg, A. Labrie, *Opt. Lett.* **13**, 961 (1988).
27. L. Wang, X. Zhu, K. G. Spears, *J. Am. Chem. Soc.* **110**, 8695 (1988); *J. Phys. Chem.* **93**, 2 (1989); P. A. Anfinrud, C. Han, T. Lian, R. M. Hochstrasser, *ibid.* **95**, 574 (1991).
28. See, for example, J. D. Beckerle *et al.* in (*23*); E. J. Heilweil, M. P. Casassa, R. R. Cavanagh, J. C. Stephenson, *Annu. Rev. Phys. Chem.* **40**, 143 (1989) and references therein.
29. H. Graener, T. Q. Lee, A. Laubereau, *J. Chem. Phys.* **90**, 3413 (1989); H. Graener, G. Seifert, A. Laubereau, *Chem. Phys. Lett.* **172**, 435 (1990); J. C. Owrutsky, Y. R. Kim, M. Li, M. J. Sarisky, R. M. Hochstrasser, *ibid.* **184**, 368 (1991).
30. R. B. Dyer, K. A. Peterson, P. O. Stoutland, W. H. Woodruff, in (*12*).
31. For a recent review of cytochrome oxidase, see B. G. Malmstrom, *Chem. Rev.* **90**, 1247 (1990).
32. R. B. Dyer, O. Einarsdóttir, P. M. Killough, J. J. López-Garriga, W. H. Woodruff, *J. Am. Chem. Soc.* 111, 7657 (1989).
33. W. H. Woodruff *et al.*, *Proc. Natl. Acad. Sci. U.S.A.* **88**, 2588 (1991).
34. Femtosecond visible absorption experiments had provided information only on the iron-porphyrin sites [P. O. Stoutland, J.-C. Lambry, J.-L. Martin, W. H. Woodruff, *J. Phys. Chem.* **95**, 6406 (1991)].
35. The instrument response may be determined from the Fe_{a_3}-CO bleach. One can also substitute a silicon wafer for the sample that, upon absorption of a visible photon, becomes reflective in the mid-IR region [R. Yen, C. V. Shank, C. Hirlimann, *Mater. Res. Soc. Symp. Proc.* **13**, 13 (1983)].
36. S. K. Doorn, P. O. Stoutland, R. B. Dyer, W. H. Woodruff, in (*12*).
37. Estimated from redox potentials for the appropriate monomer pairs; see A. Haim, *Inorg. Chem.* **14**, 113 (1985).
38. We base this on comparison to model compounds such as $[(NC)_6Fe^{III}]^{3-}$ (2118 cm^{-1}) and $[(NC)_6Fe^{II}]^{4-}$ (2044 cm^{-1}); little difference is expected for the analogous Ru complexes. See K. Nakamoto, *Infrared and Raman Spectra of Inorganic and Coordination Compounds* (Wiley, New York, ed. 4, 1986), p. 273.
39. D. Durand, L. C. Scavarda do Carmo, F. Lüty, *Phys. Rev. B* **39**, 6096 (1989).
40. We do not expect to resolve the individual states because the ground-state band itself is broad (FWHM = 23 cm^{-1}) and the spectral width of our IR probe pulse is ~8 cm^{-1} FWHM.
41. This is consistent with expectations based on recent calculations [J. Jortner and M. Bixon, *J. Chem. Phys.* **88**, 167 (1988)].
42. J. M. Robinson, M. A. Muyskens, K. J. Rensberger, F. F. Crimm, *ibid.* **93**, 3207 (1990); Z. Ma, S. D. Jons, C. F. Giese, W. R. Gentry, *ibid.* **94**, 8608 (1991); X. Xu, S.-C. Yu, R. Lingle, Jr., H. Zhu, J. B. Hopkins, *ibid.* **95**, 2445 (1991) and references therein.
43. We are preparing to address this issue directly with the use of fs Raman spectroscopy.
44. For related work on energy transfer, see: P. J. Rogers, J. I. Selco, F. S. Rowland, *Chem. Phys. Lett.* **97**, 313 (1983); P. Rogers, D. C. Montague, J. P. Frank, S. C. Tyler, F. S. Rowland, *ibid.* **89**, 9 (1982); J. D. Beckerle *et al.* in (*23*).
45. Supported by NIH grants DK36263 (W.H.W.) and GM48509 (W.H.W. and R.B.D.) as well as Los Alamos National Laboratory Directed Research grants X15D (W.H.W.) and X15B (R.B.D.). This work was performed at Los Alamos National Laboratory under the auspices of the U.S. Department of Energy.